

HIDING IMAGES INTO IMAGES WITH REAL-WORLD ROBUSTNESS

Qichao Ying^{*}, Hang Zhou[†], Xianhan Zeng^{*}, Haisheng Xu[‡], Zhenxing Qian^{*} and Xinpeng Zhang^{*}

^{*} Fudan University, [†] Simon Fraser University, [‡] NVIDIA

ABSTRACT

The existing image embedding networks are basically vulnerable to malicious attacks such as JPEG compression and noise adding, not applicable for real-world copyright protection tasks. To solve this problem, we introduce a generative deep network based method for hiding images into images while assuring high-quality extraction from the destructive synthesized images. An embedding network is sequentially concatenated with an attack layer, a decoupling network and an image extraction network. The addition of decoupling network learns to extract the embedded watermark from the attacked image. We also pinpoint the weaknesses of the adversarial training for robustness in previous works and build our improved real-world attack simulator. Experimental results demonstrate the superiority of the proposed method against typical digital attacks by a large margin, as well as the performance boost of the recovered images with the aid of progressive recovery strategy. Besides, we are the first to robustly hide three secret images.

Index Terms— image hiding, robustness, watermarking, covert communication, generative adversarial networks

1. INTRODUCTION

The development of data hiding is of increasing importance to applications such as law enforcement and military communities. Besides, information hiding can also be used in copyright protection, as one embeds information into the digital contents which can declare the ownership. In the past decades, many researches have been developed for information hiding, which can be categorized into steganography [4, 5, 6] and watermarking [1, 2, 3].

Steganography aims at embedding large-capacity data while maintaining the invariance of the statistical characteristics of the stego image by resisting steganalysis, a two-class classification task. Recently, with the rapid development of deep learning technologies, some researchers attempt to embed larger payloads into the cover images using deep neural networks, namely, hiding an image into another image (HI3). The technology is first proposed by Baluja [8] where one or multiple images can be efficiently hidden into another image called cover image using deep networks. The cover image is first processed by the preparation network to generate a high-level representation. Then, an embedding network and a reveal network are proposed for image hiding and extraction, respectively. The work soon receives extensive attentions. Some improved schemes are proposed to provide better embedding performances [9, 10, 11]. Although previous HI3 schemes [8, 9, 10, 11] have high capacities, they are not designed for robust data hiding. Once the marked image is tampered or compressed, the hidden information cannot be extracted correctly.

Watermarking focuses on robustness against possible digital attacks, such as image compression, noise adding, filtering, etc. The

technology has been widely used in copyright protection and content authentication of images in multimedia. Recently, many novel watermarking schemes with deep networks are proposed. Zhu et al. [14] proposes an end-to-end scheme for robust information hiding. The scheme is based on fully convolutional networks, which hides a fixed amount of data into a cover image. The achieved robustness is also much higher compared to traditional methods. Afterwards, robust data hiding using deep network is mainly developed for the application of digital watermarking [13, 12]. These schemes are both robust against some typical attacks such as JPEG compression, scaling and some degree of rotation. However, the payloads are significantly lower than the typical HI3 schemes. For example, [14] can only accommodate around 100 bits, while [12] only hides binary watermarks. Previously, robust watermarking has been introduced to aid many other computer vision tasks, e.g., preventing images from being inpainted [30] or reconstructed by super-resolution [31]. Ying et al. [32] uses robust data hiding to construct the immunized images. Users are able to locate tamperers and conduct self-recovery.

In the real-world applications, the users wish to apply HI3 and expect high-quality image recovery after lossy data transmission. Thus, it requires an effective method able to simultaneously embed a same-sized image while ensuring artifact imperceptibility of the synthesized image as well as strong robustness. Lately, ADH-GAN [25] is the first to ensure robustness and large capacity at the same time. However, we find that the robustness is achieved by a hybrid method of both generating an attacked training dataset and directly adding noises on the original images. Therefore, data hiding of the secret image is performed after the attacks. In real-world application, the attacks are always performed after the data embedding. As a result, the robustness of [25] cannot be achieved in real-world applications.

Motivated by the short-comings of the previous works, we propose an end-to-end generative method, which robustly hides secret images into a cover image. We jointly train an embedding network, a decoupling network, and a revealing network. A double branched U-Net [17] architecture is designed to implement the networks. We embed the secret images into the cover image. We use an improved real-world attack simulator to introduce adversarial training. On the recipient's side, we designed a decoupling network to extract the embedded residual image from the attacked image as well as recover the original cover image. Finally, the secret image can be recovered with high quality. Experimental results demonstrate that the proposed method can achieve high visual quality of both the marked and the recovered image despite the presence of different attacks. While ADH-GAN cannot hide multiple images under simple extension, we further embed two or three secret images into a cover image. The maximum payload of the proposed scheme is around 72bpp.

The main contributions of this paper are three-folded: 1) We are the first to robustly embed up to three secret images. 2) The proposed progressive image recovery method and the real-world attack simulation are effective in promoting the resilience against various digital attacks. The robustness of our scheme is superior compared to the state-of-the-art scheme. 3) Better qualities of the marked image and the recovered image can be achieved simultaneously.

This work is supported by National Natural Science Foundation of China under Grant U20B2051, U1936214. Corresponding author: Hang Zhou and Zhenxing Qian (zhouhang2991@gmail.com, zxqian@fudan.edu.cn)

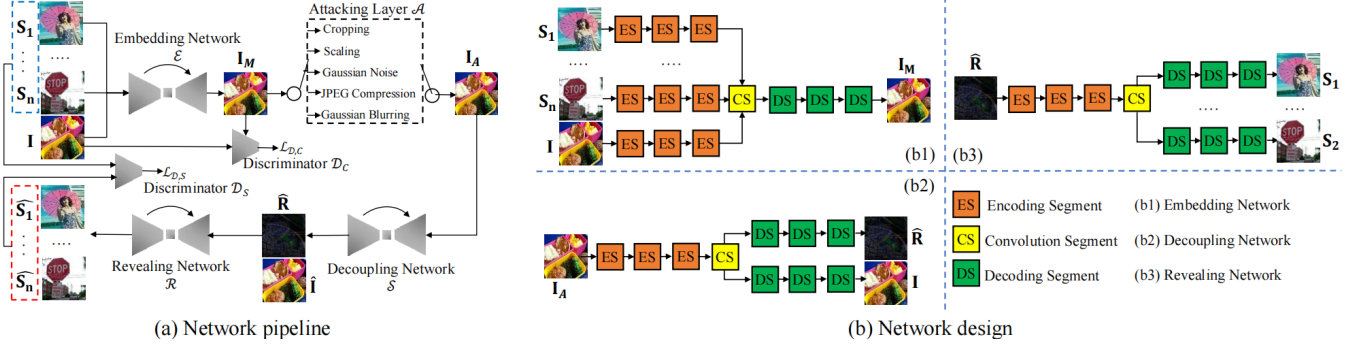


Fig. 1. Pipeline design. The embedding network hides the secret image into the cover image. The attacking layer simulates typical digital attacks. The image extraction is two-staged: we first extract the embedded residual, and then decode it into the secret image.

2. PROPOSED METHOD

Fig. 1 depicts the sketch of our proposed end-to-end deep network based HI3 method. The pipeline consists of an embedding network \mathcal{E} , an attacking layer \mathcal{A} , a decoupling network \mathcal{S} , a revealing network \mathcal{R} and two discriminators \mathcal{D}_C and \mathcal{D}_S . We propose a novel multi-branched U-Net architecture to implement \mathcal{E} , \mathcal{S} and \mathcal{R} . The discriminators are to respectively monitor the quality of the marked images and the extracted images. We use Patch-GAN [19] as the discriminators.

2.1. Image embedding pipeline

We use the embedding network \mathcal{E} to hide one or more secret images $\mathbf{S} = \{\mathbf{S}_1, \dots, \mathbf{S}_n\}$ into a cover image \mathbf{I} . n denotes the number of secret images and we let $n \in [1, 3]$. A residual image \mathbf{R} is generated by \mathcal{E} and the marked image \mathbf{I}_M is produced by adding the residual image on the cover image, i.e., $\mathbf{I}_M = \mathbf{I} + \mathbf{R}$. The residual image can be viewed as a compressed version of \mathbf{S} . We extend the typical U-Net architecture by introducing multiple (n) independent encoding parts that respectively generate features for the cover image \mathbf{I} and the secret image \mathbf{S} . These branches do not share weights. Fig. 1(b1) shows an example of \mathcal{E} where there are two secret images and therefore three encoding branches. In the decoding part, the features from the branches are all concatenated with the output of the previous layer. The main advantage of this design compared to the original U-Net structure is that the relevance of the features from the secret images and the cover image can be disentangled and more efficiently utilized in generating an indistinguishable marked image with improved robustness.

2.2. Improved Attack Simulation for Real-World Robustness

We build the attacking layer \mathcal{A} that attacks the marked image \mathbf{I}_M as a way of adversarial training. Similar to [14, 12], the common digital attacks are simulated by differentiable methods. The attacking layer contains five types of typical digital attacks, namely, the addition of Gaussian noise, the Gaussian blurring, the random scaling, the lossy JPEG compression and the random cropping. We take the implementation from [14] except: 1) we build our own JPEG simulator. 2) JPEG compression attack is always present, i.e., the other attacks are further conducted on the JPEG compressed image.

Though many schemes have already proposed a variety of JPEG simulators, e.g., JPEG-SS [33], JPEG-Mask [14], MBRS [34], it is

reported that the real-world JPEG robustness is still far from satisfactory. We analyze that the reason is mainly two-folded: 1) the networks will finally over-fit a fixed JPEG simulator, resulting in poor performance in blind JPEG artefact removal. 2) other attacks such as rescaling maintain way more clues (\mathbf{R}) compared to JPEG compression. As a result, when the attacks are iteratively performed, the networks will sacrifice robustness against JPEG for the rest.

To address the first issue, we propose to conduct a similar instance-agnostic JPEG interpolation, inspired by Mix-up [29] which uses label interpolation for data augmentation in classification tasks. We construct the simulated JPEG image using different implementations and quality factors as follows:

$$\mathbf{I}_{jpg} = \sum_{\mathcal{J}_k \in \mathcal{J}} \sum_{QF_l \in [10, 100]} \epsilon \cdot \mathcal{J}_k(\mathbf{I}_M, QF_l), \quad (1)$$

where $\sum_{\mathcal{J}_k \in \mathcal{J}} \epsilon = 1$, $\mathcal{J} \in \{\text{JPEG-SS, JPEG-Mask, MBRS}\}$ and QF stands for the quality factor. To address the second issue, when we train the network to be robust against the attacks other than JPEG compression, we performed the attacks on \mathbf{I}_{jpg} instead of directly on \mathbf{I}_M , where we fix all of the QF_l in (1) to be 90.

2.3. Progressive image recovery pipeline

Besides the improved JPEG simulator, we propose to progressively recover the secret by extracting the embedded residual $\hat{\mathbf{R}}$ first. Successful image recovery from the attacked image has long been a difficult task to achieve for many previous schemes using straight-forward image recovery [8, 9, 10]. From the observation that the information of the hidden secret images \mathbf{S} within the cover image \mathbf{I} can only be reconstructed by the residual image \mathbf{R} , we begin the progressive image recovery by first extract as well as augment the embedded residual image as $\hat{\mathbf{R}}$.

We train a decoupling network \mathcal{S} to extract $\hat{\mathbf{R}}$ ahead of the recovery of the secret images \mathbf{S} . During training stage, the decoupling network \mathcal{S} has access to both the original embedded residual image \mathbf{R} and the attacked image \mathbf{I}_A . Therefore, the network knows the difference between them and is able to learn a function to approximately transform \mathbf{I}_A into $\hat{\mathbf{R}}$. Considering that the residual image \mathbf{R} is usually weak, we encourage $\hat{\mathbf{R}}$ to be as close as possible as $5 \times \mathbf{R}$. We believe the augmentation can help improving the learning performance. We also demand \mathcal{S} to recover the original image to aid residual extraction.

Afterwards, we feed the revealing network \mathcal{R} with $\hat{\mathbf{R}}$ and recover the secret image $\hat{\mathbf{S}}$. $\hat{\mathbf{S}} = \{\hat{\mathbf{S}}_1, \dots, \hat{\mathbf{S}}_n\}$. We also build \mathcal{S} and \mathcal{R} on

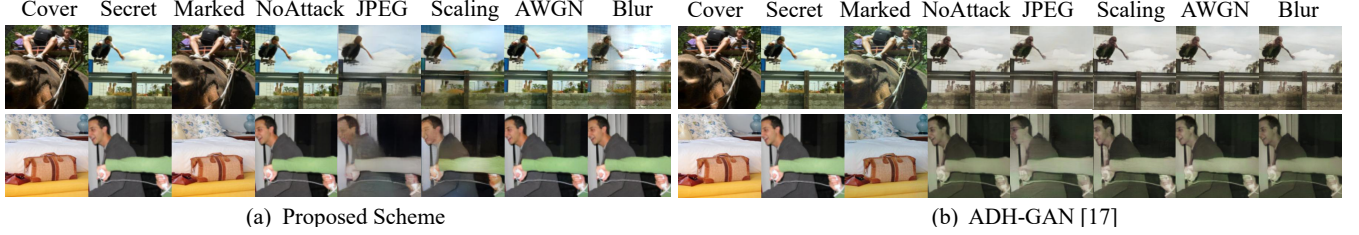


Fig. 2. Comparison of robustness against various kinds of attacks.

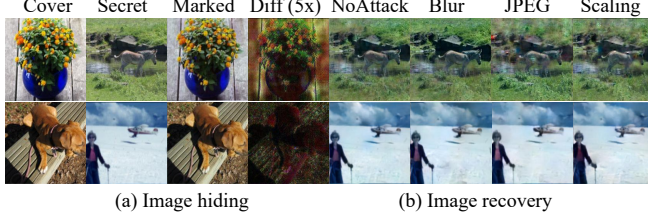


Fig. 3. Image embedding and extraction test of hiding one secret image. The difference is augmented for better illustration.

Table 1. Performance comparison of image extraction over 1000 test images. (First row: PSNR. Second row: SSIM)

Method	NoAttack	JPEG	Scaling	Blur	C&W
Proposed	29.76	26.69	28.47	28.32	26.73
	0.916	0.875	0.895	0.905	0.863
ADH-GAN [25]	25.22	17.64	17.41	14.63	16.58
	0.867	0.634	0.625	0.498	0.588

top of the proposed multi-branch U-Net architecture. Fig. 1(b2,b3) shows an example. The difference compared to \mathcal{E} is that we build n branches for \mathcal{R} and two branches for \mathcal{S} in the decoding parts, while for each network there is only one shared encoding part.

2.4. Objective loss function

We encourage the marked image \mathbf{I}_M and the extracted image \mathbf{I}_R to respectively resemble the targeted image \mathbf{I} and the secret image \mathbf{S} . Besides, we encourage \mathbf{S} to approximately reconstruct \mathbf{I} . Therefore, the reconstruction loss is $\mathcal{L}_{rec} = \mathcal{F}(\mathbf{I}, \mathbf{I}_M) + \mathcal{F}(\mathbf{S}, \hat{\mathbf{S}}) + \mathcal{F}(\mathbf{I}, \hat{\mathbf{I}})$, where \mathcal{F} is the ℓ_2 distance. The adversarial loss is to further control the introduced distortion by fooling the discriminator. For the discriminative loss $\mathcal{L}_{dis,C}$ and $\mathcal{L}_{dis,R}$, we accept the least squared adversarial loss (LS-GAN) [26]. Note that we train a unified \mathcal{D}_R to distinguish \mathbf{S} from $\hat{\mathbf{S}}$. Finally, the reconstruction loss for the extracted residual image is $\mathcal{L}_S = \|\mathbf{5} \cdot \mathbf{R} - \hat{\mathbf{R}}\|_2^2$. The total loss for the proposed scheme is $\mathcal{L}_G = \mathcal{L}_{rec} + \alpha \cdot \mathcal{L}_{dis,C} + \beta \cdot \mathcal{L}_{dis,R} + \gamma \cdot \mathcal{L}_S$, where α, β and γ are hyper-parameters.

3. EXPERIMENTS

We train the scheme on the COCO training/test set [22]. We resize the images to the size of 256×256 . The hyper-parameters are set as $\alpha = 0.05, \beta = 0.05, \gamma = 1.5$. The batch size is set as four. We find a larger batch size will jeopardize the networks from generalizing the learned robustness. The payload of the proposed

scheme depends on the number of the hidden secret images, i.e., 48bpp (bit per pixel) when $n = 2$ and 72bpp when $n = 3$. We use Adam optimizer [37] with the default parameters. The learning rate is 2×10^{-4} . The embedding rate of the state-of-the-art robust HI3 scheme (ADH-GAN [25]) is 24bpp. Therefore, we begin our evaluation with hiding one image ($n = 1$). Then we discuss on hiding multiple images ($n > 1$). While ADH-GAN cannot hide multiple images under simple extension, we further embed two or three secret images into a cover image using our method.

3.1. Robustly Hiding One Image

Imperceptibility and Robustness. In Fig. 2 and Fig. 3, we arbitrarily select four pairs of images for illustration. The differences are augmented five times for better illustration. We can observe that the embedding of the secret image on the marked images is imperceptible to human eyes. The difference \mathbf{D} is imperceptible. Little detail of the watermark can be found. We have conducted more embedding experiments over 1000 images and the average PSNR between the marked images and the cover images is 33.94dB. The average SSIM [24] is 0.9517. In Fig. 3, we further apply different attacks on the marked images. The results are promising. We can clearly observe that the overall image quality of the extracted images is high, which does not downgrade much despite the presence of the attacks. The reason why the secret image cannot be losslessly extracted even when there is not attack is because of the adversarial training. The networks are frequently exposed to attacks and therefore they jointly learn a robust but not accurate way of image reconstruction. One can train his one networks without using the attacking layer in an attack-free environment.

Comparison with ADH-GAN. In Fig. 2, we compare our method with [25] on both robustness and imperceptibility. First, there exists color inconsistency in the marked image produced by [25], which is also a problem for many previous works [8, 14]. However in our scheme, this phenomenon rarely occurs. We analyze that for successful data extraction, the data hiding networks sometimes weaken the strength of the targeted image apart from strengthening the embedded signal. Such occurrence can be largely lowered by penalizing a larger image reconstruction loss. However, the data extraction performance will be much worse. Second, we can observe that in the extracted images of [25], there is visual artifact both in color and in texture. In contrast, our scheme can largely preserve image fidelity without hallucinating image details. For space limit, please zoom in for a closer scrutiny. We proceed our comparison by randomly selecting 1000 pairs of images and apply various kinds of attacks. For JPEG compression, we take $QF = 70$ as an example. The average performances of the proposed scheme and [25] are reported in Table 1. Note that unlike [14], the performances are from one model trained with multiple kinds of attacks instead of from separate specified models. The average SSIMs of the recovered image produced by

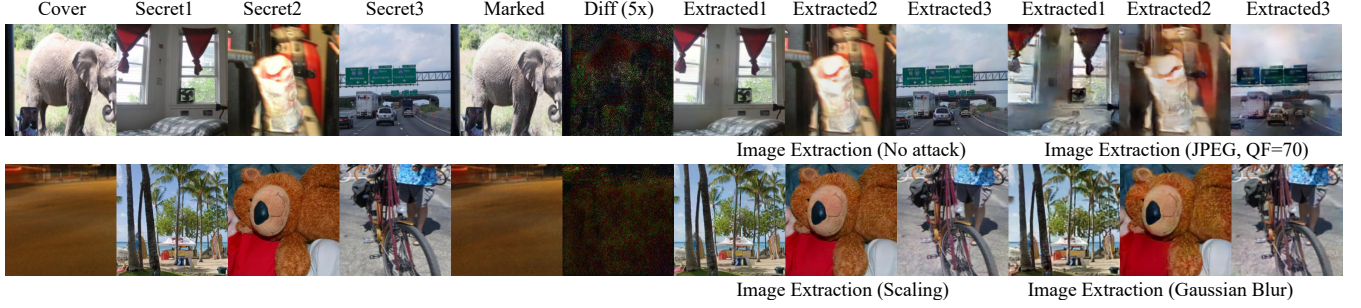


Fig. 4. Comparison of robustness against different attack among different methods. “GT” stands for the ground-truth image.

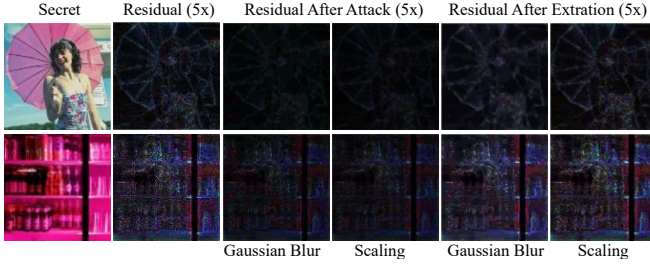


Fig. 5. Examples of the extracted residual images. The embedded residual images are largely destroyed by the attacks. The decoupling network successfully augments them.

Table 2. Ablation study of image extraction with JPEG QF=70.

Configuration	PSNR	SSIM
Without progressive recovery	13.66	0.612
Without any discriminator	15.37	0.726
Implementing \mathcal{E} using traditional U-Net	18.16	0.817
Without the proposed JPEG simulator	23.95	0.839
Fully implemented	26.68	0.875

Table 3. Performance of image extraction on hiding multiple images. The payload varies from 24bpp ($n = 1$) to 72bpp ($n = 3$)

n	NoAttack	JPEG	Scaling	Blur	AWGN	C&W
2	28.62	24.60	26.58	26.82	25.01	26.71
	0.889	0.824	0.873	0.854	0.793	0.847
3	28.14	23.02	24.59	24.22	22.78	24.13
	0.862	0.757	0.854	0.844	0.735	0.806
4	23.79	17.81	19.17	16.00	13.64	18.93
	0.805	0.664	0.737	0.547	0.511	0.677

the proposed method are generally above 0.8 despite the variety of added attacks. C&W [28] is a famous adversarial example (AE) algorithm that the networks are not trained against. The robustness can be generalized against adversarial attacks. By comparison, the average performance of [25] is worse than that of the proposed method. The result is consistent with Fig. 2 which proves that the proposed method has better imperceptibility and robustness in image hiding.

Validation of the Pipeline Design. We begin with analyzing what the decoupling network \mathcal{S} can learn. Fig. 5 shows two examples

where the embedding network \mathcal{E} encodes the secret images (first column) into the residual images (second column) and adds them onto the cover images (not shown). In the third and fourth column, we show how the traditional attacks destroy the embedded residual image. However, after running \mathcal{S} , we can clearly observe that the extracted residual images are much close to the original residual images. Through the comparison, we prove that the decoupling network can effectively reconstruct the added residual images, which are crucial in recovering the secret images.

Then, we verify the effectiveness of several components in the scheme. In Table. 2, we show the experimental results of several ablation tests. In each test, we train the modified pipeline using the same learning rates and optimizers. We stop the training until the reconstruction loss of the marked image in each test is close to that of the fully implemented proposed method, and the recovery loss cannot be further minimized. The results show that every component plays an important role.

3.2. Robustly Hiding Two or Three Images

Fig. 4 shows three groups of results on hiding three secret images. We see that the distortion introduced on the cover image is significantly and understandably larger than that on hiding a single image. Also, the residual images are no longer easily interpretable. But overall, the image quality of the marked image and the extracted images are high. Besides, we can barely observe one extracted image from another, indicating the extracted images are well disentangled.

Table. 3 shows the average results of 1000 groups of images on hiding two or three images. We retrain the networks with different amount of secret images. The average PSNR of the marked image is 32.13dB when $n = 2$ and 32.69dB when $n = 2$. We see that the image quality of the extracted images can be preserved. We also find that the performance does not drop much when we hide three images compared to Table.1. However, the performance significantly drops when we tend to hide a fourth secret image. Therefore, we believe the maximum payload of the proposed scheme is around 72bpp.

4. CONCLUSION

This paper presents a new method for hiding images into images with real-world robustness. We propose an embedding network to conceal secret images into a cover image, where the introduced perturbation is close to imperceptible. We propose an improved attack simulator and progressively recover the hidden images. The comprehensive experiments prove that compared to the state-of-the-art methods, the proposed method can simultaneously embed a larger payload, ensure the visual effect of the marked image and offer a much stronger robustness.

5. REFERENCES

- [1] Jinyuan Tao, Sheng Li, Xinpeng Zhang, and Zichi Wang, "Towards robust image steganography," *IEEE Transactions on Circuits and Systems for Video Technology*, vol. 29, no. 2, pp. 594–600, 2018.
- [2] Vahid Sedighi, Rémi Cogranne, and Jessica Fridrich, "Content-adaptive steganography by minimizing statistical detectability," *IEEE Transactions on Information Forensics and Security*, vol. 11, no. 2, pp. 221–234, 2015.
- [3] Kejiang Chen, Hang Zhou, Wenbo Zhou, Weiming Zhang, and Nenghai Yu, "Defining cost functions for adaptive jpeg steganography at the microscale," *IEEE Transactions on Information Forensics and Security*, vol. 14, no. 4, pp. 1052–1066, 2018.
- [4] Han Fang, Weiming Zhang, Hang Zhou, Hao Cui, and Nenghai Yu, "Screen-shooting resilient watermarking," *IEEE Transactions on Information Forensics and Security*, vol. 14, no. 6, pp. 1403–1418, 2018.
- [5] Namita Agarwal, Amit Kumar Singh, and Pradeep Kumar Singh, "Survey of robust and imperceptible watermarking," *Multimedia Tools and Applications*, vol. 78, no. 7, pp. 8603–8633, 2019.
- [6] Md Asikuzzaman and Mark R Pickering, "An overview of digital video watermarking," *IEEE Transactions on Circuits and Systems for Video Technology*, vol. 28, no. 9, pp. 2131–2153, 2017.
- [7] Yun-Qing Shi, Xiaolong Li, Xinpeng Zhang, Hao-Tian Wu, and Bin Ma, "Reversible data hiding: advances in the past two decades," *IEEE access*, vol. 4, pp. 3210–3237, 2016.
- [8] Shumeet Baluja, "Hiding images in plain sight: Deep steganography," *Advances in Neural Information Processing Systems*, vol. 30, pp. 2069–2079, 2017.
- [9] Shumeet Baluja, "Hiding images within images," *IEEE Transactions on Pattern Analysis and Machine Intelligence*, 2019.
- [10] Xintao Duan, Kai Jia, Baoxia Li, Daidou Guo, En Zhang, and Chuan Qin, "Reversible image steganography scheme based on a u-net structure," *IEEE Access*, vol. 7, pp. 9314–9323, 2019.
- [11] Rafia Rahim, Shahroz Nadeem, et al., "End-to-end trained cnn encoder-decoder networks for image steganography," in *Proceedings of the European Conference on Computer Vision (ECCV)*, 2018, pp. 0–0.
- [12] Seung-Min Mun, Seung-Hun Nam, Haneol Jang, Dongkyu Kim, and Heung-Kyu Lee, "Finding robust domain from attacks: A learning framework for blind watermarking," *Neuro-computing*, vol. 337, pp. 191–202, 2019.
- [13] Haribabu Kandi, Deepak Mishra, and Subrahmanyam RK Sai Gorthi, "Exploring the learning capabilities of convolutional neural networks for robust image watermarking," *Computers & Security*, vol. 65, pp. 247–268, 2017.
- [14] Jiren Zhu, Russell Kaplan, Justin Johnson, and Li Fei-Fei, "Hidden: Hiding data with deep networks," in *Proceedings of the European conference on computer vision (ECCV)*, 2018, pp. 657–672.
- [15] Xiyang Luo, Ruohan Zhan, Huiwen Chang, Feng Yang, and Peyman Milanfar, "Distortion agnostic deep watermarking," in *Proceedings of the IEEE/CVF Conference on Computer Vision and Pattern Recognition*, 2020, pp. 13548–13557.
- [16] Xiuli Bi, Yanbin Liu, Bin Xiao, Weisheng Li, Chi-Man Pun, Guoyin Wang, and Xinbo Gao, "D-unet: A dual-encoder u-net for image splicing forgery detection and localization," *arXiv preprint arXiv:2012.01821*, 2020.
- [17] Olaf Ronneberger, Philipp Fischer, and Thomas Brox, "U-net: Convolutional networks for biomedical image segmentation," in *International Conference on Medical image computing and computer-assisted intervention*. Springer, 2015, pp. 234–241.
- [18] Christian Szegedy, Vincent Vanhoucke, Sergey Ioffe, Jon Shlens, and Zbigniew Wojna, "Rethinking the inception architecture for computer vision," in *Proceedings of the IEEE conference on computer vision and pattern recognition*, 2016, pp. 2818–2826.
- [19] Phillip Isola, Jun-Yan Zhu, Tinghui Zhou, and Alexei A Efros, "Image-to-image translation with conditional adversarial networks," in *Proceedings of the IEEE conference on computer vision and pattern recognition*, 2017, pp. 1125–1134.
- [20] Justin Johnson, Alexandre Alahi, and Li Fei-Fei, "Perceptual losses for real-time style transfer and super-resolution," in *European conference on computer vision*. Springer, 2016, pp. 694–711.
- [21] Leonid I Rudin, Stanley Osher, and Emad Fatemi, "Nonlinear total variation based noise removal algorithms," *Physica D: nonlinear phenomena*, vol. 60, no. 1-4, pp. 259–268, 1992.
- [22] Tsung-Yi Lin, Michael Maire, Serge Belongie, James Hays, Pietro Perona, Deva Ramanan, Piotr Dollár, and C Lawrence Zitnick, "Microsoft coco: Common objects in context," in *European conference on computer vision*. Springer, 2014, pp. 740–755.
- [23] Jia Deng, Wei Dong, Richard Socher, Li-Jia Li, Kai Li, and Li Fei-Fei, "Imagenet: A large-scale hierarchical image database," in *2009 IEEE conference on computer vision and pattern recognition*. Ieee, 2009, pp. 248–255.
- [24] Zhou Wang, Alan C Bovik, Hamid R Sheikh, and Eero P Simoncelli, "Image quality assessment: from error visibility to structural similarity," *IEEE transactions on image processing*, vol. 13, no. 4, pp. 600–612, 2004.
- [25] Chong Yu, "Attention based data hiding with generative adversarial networks," in *Proceedings of the AAAI Conference on Artificial Intelligence*, 2020, vol. 34, pp. 1120–1128.
- [26] Xudong Mao, Qing Li, Haoran Xie, Raymond YK Lau, Zhen Wang, and Stephen Paul Smolley, "Least squares generative adversarial networks," in *Proceedings of the IEEE international conference on computer vision*, 2017, pp. 2794–2802.
- [27] Sergey Ioffe and Christian Szegedy, "Batch normalization: Accelerating deep network training by reducing internal covariate shift," in *International conference on machine learning*. PMLR, 2015, pp. 448–456.
- [28] Nicholas Carlini and David Wagner, "Towards evaluating the robustness of neural networks," in *2017 IEEE Symposium on Security and Privacy (SP)*. IEEE, 2017, pp. 39–57.
- [29] Hongyi Zhang, Moustapha Cisse, Yann N Dauphin, and David Lopez-Paz, "mixup: Beyond empirical risk minimization," *arXiv preprint arXiv:1710.09412*, 2017.
- [30] David Khachaturov, Ilia Shumailov, Yiren Zhao, Nicolas Papernot, and Ross Anderson, "Markpainting: Adversarial machine learning meets inpainting," *arXiv preprint arXiv:2106.00660*, 2021.

- [31] Minghao Yin, Yongbing Zhang, Xiu Li, and Shiqi Wang, “When deep fool meets deep prior: Adversarial attack on super-resolution network,” in *Proceedings of the 26th ACM international conference on Multimedia*, 2018, pp. 1930–1938.
- [32] Qichao Ying, Zhenxing Qian, Hang Zhou, Haisheng Xu, Xinpeng Zhang, and Siyi Li, “From image to imuge: Immunized image generation,” in *Proceedings of the 29th ACM international conference on Multimedia*, 2021, pp. 1–9.
- [33] Kunlin Liu, Dongdong Chen, Jing Liao, Weiming Zhang, Hang Zhou, Jie Zhang, Wenbo Zhou, and Nenghai Yu, “Jpeg robust invertible grayscale,” *IEEE Transactions on Visualization and Computer Graphics*, 2021.
- [34] Zhaoyang Jia, Han Fang, and Weiming Zhang, “Mbrs: Enhancing robustness of dnn-based watermarking by mini-batch of real and simulated jpeg compression,” *arXiv preprint arXiv:2108.08211*, 2021.
- [35] Djork-Arné Clevert, Thomas Unterthiner, and Sepp Hochreiter, “Fast and accurate deep network learning by exponential linear units (elus),” *arXiv preprint arXiv:1511.07289*, 2015.
- [36] Fisher Yu and Vladlen Koltun, “Multi-scale context aggregation by dilated convolutions,” *arXiv preprint arXiv:1511.07122*, 2015.
- [37] Diederik P Kingma and Jimmy Ba, “Adam: A method for stochastic optimization,” *arXiv preprint arXiv:1412.6980*, 2014.
- [38] HD Cheng and XJ Shi, “A simple and effective histogram equalization approach to image enhancement,” *Digital signal processing*, vol. 14, no. 2, pp. 158–170, 2004.
- [39] Andrés Bruhn, Joachim Weickert, and Christoph Schnörr, “Lucas/kanade meets horn/schunck: Combining local and global optic flow methods,” *International journal of computer vision*, vol. 61, no. 3, pp. 211–231, 2005.